Available online at www.sciencedirect.com
SCIENCE DIRECT®
Biochemical and Biophysical Research Communications 329 (2005) 32–39
BBRC
www.elsevier.com/locate/ybbrc

Identification of novel Nox4 splice variants with impact on ROS levels in A549 cells

Parag Goyal [a], Norbert Weissmann [a], Frank Rose [a], Friedrich Grimminger [a], Hans J. Schäfers [b], Werner Seeger [a], Jörg Hänze [a,*]

[a] Department of Internal Medicine, Medical School University of Giessen, Klinikstr. 36, D-35392 Giessen, Germany
[b] Department of Thorax and Heart Surgery, Medical School University Saarland/Bad Homburg, Gebäude 56, 66421 Homburg/Saar, Germany

Received 10 January 2005
Available online 1 February 2005

Abstract

NAD(P)H oxidases (Nox) generate reactive oxygen species (ROS) that function in host defense and cellular signaling. While analyzing the expression of Nox4 at the protein and the mRNA levels, we identified four novel Nox4 splice-variants Nox4B, Nox4C, Nox4D, and Nox4E, which are expressed in human lung A549 cell line and lung tissues. One Nox4 isoform lacks the first NAD(P)H binding site (Nox4B) while another lacks all FADH and NAD(P)H binding sites (Nox4C). Cells over-expressing NoxB or Nox4C exhibited a decrease in ROS levels. Thus, these isoforms have dominant negative characteristics for ROS generation. Two other splice-variants (Nox4D, Nox4E) lack the transmembrane domains, suggesting these as non-membrane associated isoforms. Nox4D contains all FADH and NAD(P)H binding domains and shows the same rate of ROS generation as Nox4 prototype. Taken together, we suggest that Nox4 exists as several isoforms that may have different functions in ROS-related cell signaling.

Keywords: NAD(P)H oxidase; Nox4; Nox1; Splice variant; ROS signaling

Reactive oxygen species (ROS) are generated enzymatically by NAD(P)H oxidases [1,2], mitochondria [3], xanthine oxidase [4], and under certain conditions by endothelial nitric oxide synthase [5]. The ROS are involved in diverse biological processes including host defense [1], signal transduction [6], oxygen sensing [7], proliferation, apoptosis, and response to mechanical strain [8]. They also control gene regulatory pathways mediated by antioxidant-responsive-element via mitogen-activated protein (MAP) kinase [9] or hypoxia-responsive-element via hypoxia-inducible factor (HIF) [10,11]. The activation of ROS metabolism has been associated with inflammation, vascular atherosclerosis [12], diabetes [13], hypertension [14], and tumorigenesis [15].

The family of NAD(P)H oxidases (Nox/Duox) consists of Nox1, Nox2 ($gp91^{phox}$), Nox3, Nox4, Nox5 as well as the Duox1 and Duox2 [16], which contain additional extracellular peroxidase domains and calcium binding domains. The Nox1–4 members share considerable homology and contain five or six transmembrane domains. This region also contains conserved histidine residues that coordinate binding of a Fe^{2+} heme group that mediates electron flow from NAD(P)H to oxygen. The C-terminal region is intracellular and exhibits regions of homology with other FAD binding proteins. This region also contains four domains exhibiting homology with pyridine nucleotide binding proteins that interact with NAD(P)H.

The NAD(P)H oxidases are expressed in a tissue and cell-type specific manner. Originally, $gp91^{phox}$ was found

* Corresponding author. Fax: +49 641 9942429.
E-mail address: joerg.haenze@innere.med.uni-giessen.de (J. Hänze).

0006-291X/$ - see front matter © 2005 Elsevier Inc. All rights reserved.
doi:10.1016/j.bbrc.2005.01.089

in phagocytes [17]. gp91^{phox} is the best-characterized member of the family and interacts with the membrane bound p22^{phox} comprising the flavocytochrome b_{558}. This core unit interacts with various cytosolic regulating and activating subunits p47^{phox}, p67^{phox}, p40^{phox}, and rac being recruited upon activation [18].

Recently, the related Nox1, Nox3, and Nox4 have been cloned [15,16,19]. Two further homologues of p47^{phox} and p67^{phox} named NoxO1 and NoxA1 have been isolated and were shown strongly to enhance ROS generation when coexpressed with Nox1 [20]. However, none of these subunits have been demonstrated to interact with Nox4.

The localization and assembly of new Nox subtypes is not known and is inferred from studies of the gp91^{phox} form in phagocytes. One cytochemical study shows immunostaining of Nox1 on the plasma membrane while Nox4 surprisingly is detected mainly in nucleus [21]. Furthermore, whether ROS are released intra- or extracellularly is not known for the non-gp91^{phox} members.

When analyzing the Nox4 expression on both protein and mRNA levels in A549 cell line, and on mRNA level in human lung tissue and pulmonary vessel cells, we observed several Nox4 isoforms in addition to Nox4 prototype, which were expressed in significant expression rates. The presence of splice variants for Nox4 has been documented earlier with the two independent NCBI database entries XP208058 and AY288918. Using shotgun-cloning approach, four isoforms were cloned. Sequencing data revealed three new Nox4 splice-variants and one similar to the previously reported Nox4 variant (AY288918), with differences in domains that have critical functions. Strikingly, two of these isoforms lacked one NAD(P)H or all NAD(P)H and FADH binding sites, and suppressed ROS generation. Another striking variant lacked all transmembrane domains and exhibited the same potency of ROS generation, as did Nox4 prototype. In this study, we describe the structural organization and sub-cellular localization of these isoforms. We analyzed their ROS-generating properties in comparison with those of Nox1.

Materials and methods

Cell culture and transfection. The A549 human pulmonary epithelial cell line and HEK 293 human embryonic kidney cell line were maintained according to the protocol of the American Type Culture Collection. Plasmid DNA was transfected by cationic lipids (Lipofectamine 2000) according to the manufacturer's protocol (Invitrogen, Carlsbad, USA).

Human lung tissue. Healthy donor lung tissue not utilizable for transplantation was processed in accordance with national and university regulations. Lung tissue sections and vessels were prepared from fresh lungs and frozen in liquid nitrogen.

RNA-extraction and RT-PCR: Total RNA was extracted and RT-PCR performed as described [10]. The following primers were used: Nox4 (derived from EMBL Acc. No: BC040105), forward (containing improved Kozak sequence, underlined): 5′ GCCGCCGCCATGGC TGTGTCCTGG 3′ reverse: 5′ GGCATAACACAGCTGATTGA TTCCGCTGAG 3′. HPRT (derived from NCBI Acc.No: NM_000194), forward: 5′ TCGAGATGTGATGAAGGAGATG GGA 3′ reverse: 5′ TCAAATCCAACAAAGTCTGGCTTAT 3′. The thermal cycler program used was (95 °C, 15 m, followed by 40 cycles: 94 °C, 15 s, 58 °C, 30 s and 72 °C, 2 min, and 72 °C, 10 min).

Construction of plasmids recombinant for Nox4 isoforms and Nox1. For cloning of the Nox4 variants, we performed RT-PCR using RNA extracts from the A549 cells and the same primers as described in RT-PCR section. Purified PCR products were ligated into pGEM-Teasy plasmid (Promega) and the clones were sequenced. The inserts were subcloned into pcDNA3.1 expression plasmid (Invitrogen) and a modified pCMV plasmid (Clontech) with a hemagglutinin A (HA) tag in-frame at the C-terminus using *Not*I restriction site. The Nox1 expression vector based on pcDNA3.1 plasmid was employed as described [10].

Western-blot. Western-blot analysis for the HA-tag and for Nox4 was performed using monoclonal mouse antibody against HA (Sigma–Aldrich) and an antibody was raised in rabbit against a synthetic peptide corresponding to position 556–569: LHKLSNQNNSYGTR of the Nox4 protein (GenBank Accession No. NP_058627). This antibody was purified by affinity chromatography by coupling of the peptide used for immunization. Cells were lysed using Laemmli buffer and denatured for 5 min at 95 °C. Samples were run on a SDS–PAGE gel for Western-blot as described [10]. HA or Nox4 antibodies were added at dilutions of 1:10,000 and 1:2000, respectively. For blocking of the Nox4 antibody, Nox4 peptide was added at a concentration of 20 μg/ml to the antibody solution for 3 h. As a control a non-related peptide of the same length was used. Specific immunoreactive signals were detected employing a chemiimager (FluorChem 8900, Alpha Innotech).

Immunocytochemistry. Cells were cultured on chamber slides, treated as indicated, fixed in acetone and methanol (1:1), and blocked with 5% (m/v) BSA in phosphate-buffered saline (PBS) for 30 min followed by incubation for 1 h with HA (1:500) antibody diluted in 0.1% (m/v) BSA in PBS. Indirect immunofluorescence was obtained by incubation with FITC-conjugated anti-mouse (Dako, Denmark) antibody diluted 1:100 in 0.1% (m/v) BSA in PBS for 1 h. Cells were stained for DAPI (1:100 in 0.1% (m/v) BSA in PBS).

ROS measurement. Intracellular ROS concentration was measured using 2′,7′-dichlorofluorescein diacetate (DCFH-DA, Sigma–Aldrich, St. Louis, USA) and a spectrofluorometer (FL-600, BIO-TEK Instruments, Winooski, USA) as described [10]. Values are given as relative induction of fluorescence at 535 nm compared to control vector-transfected cell. Background fluorescence was taken into account by subtracting values of fluorescence derived from wells without cells.

Bioinformatic analysis. Sequence analysis was performed using CLUSTAL and PSORT II from Heidelberg UNIX Sequence analysis resources (HUSAR software package).

Results

Expression analysis of Nox4 on protein and mRNA level

Analysis of Nox4 protein expression in human lung A549 cells by Western-blot using Nox4 specific antibody demonstrated several bands between 20 and 70 kDa (Fig. 1A). The specificity of these bands due to Nox4 antibody and not due to secondary antibody was confirmed since co-incubation of Nox4 antibody with

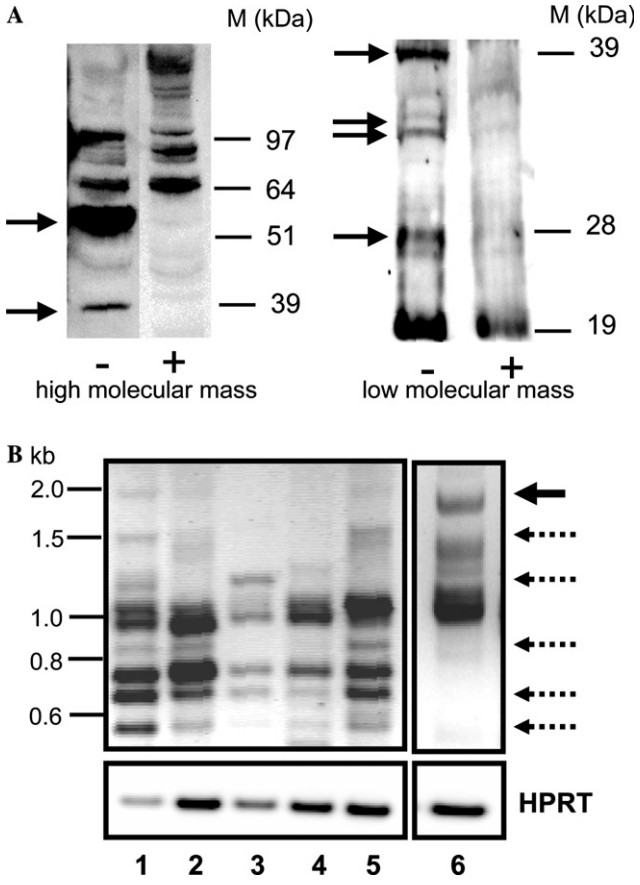

Fig. 1. (A) Nox4 Western-blot analysis of A549 cells. Nox4 antibody was blocked by preincubation with a Nox4 peptide used for immunization (+) or non-related peptide (−). Arrows represent specific Nox4 immunoreactive bands. The left part shows the high molecular mass range and the right part shows the lower molecular mass range (size marker: M). (B) RT-PCR analysis of RNA extracts from A549 cells (1), primary cultured cells from pulmonary artery adventitial fibroblasts (2), and tissue extracts of pulmonary artery (3), pulmonary vein (4), lung tissue (5), and HEK 293 cells (6) (size marker in kilobases, kb). The upper boxes represent RT-PCR analysis using Nox4 full-length primers and lower boxes represent RT-PCR using HPRT primers. Bold arrow indicates the expected full length Nox4 cDNA while dotted arrows indicate bands that differ between tissue types.

Nox4 derived peptide (against which the antibody was raised) abrogated antibody binding. In addition, we performed mRNA expression analysis by RT-PCR. Several smaller bands in addition to Nox4 prototype (~1.8 kb) were observed in A549 cells. Some of these bands were also observed in RNA extracts from homogenates of pulmonary artery, pulmonary veins, cultured primary pulmonary artery adventitial fibroblasts, and lung (Fig. 1B). The expression profiles of these bands were also observed to be different between one tissue type and another when compared with expression for housekeeping gene HPRT. As Nox4 was originally identified in kidney, we also performed mRNA expression analysis of RNA extracts from HEK 293 cells. In kidney, bands were observed only between 1 and 1.8 kb range (including full length) and no smaller bands were observed.

Structural organization of Nox4 isoforms

For further characterization of these bands, we performed cloning and sequencing of Nox4 RT-PCR products and isolated four new Nox4 splicing variants. The exon structure (Fig. 2) and the alignment of derived amino acid sequences with corresponding functional domains are shown (Fig. 3). Variant B also described in another database entry (Accession No. AY288918) revealed splicing of exon 14 resulting in the lack of the first NAD(P)H binding site in the protein. Variant C is a result of splicing of exons 9–11, which generates a frame shift in mRNA, and hence a new stop codon in the beginning of exon 12. Consequently, this variant does not contain any FADH or NAD(P)H binding sites in protein. Variants D and E are both a consequence of splicing of exons 3–11 whereas variant E has an additional splicing of exon 14. These two variants have only the first transmembrane domain, which is followed by N-terminal signal peptide cleavage site. Variant D contains all FADH and NAD(P)H binding sites, whereas variant E additionally lacks one NAD(P)H binding site similar to variant B.

Transient overexpression of tagged Nox4 isoforms and subcellular localization of Nox4 by immunocytochemistry

For functional characterization, we subcloned the Nox4 isoforms into expression plasmid. Since not all variants were detectable by our Nox4 antibody, which is targeted to the C-terminus of the prototype, we also tagged these isoforms with HA-tag at the C-terminus of the protein. The expression of these variants after transfection into A549 cells is shown by HA Western-blot (Fig. 4A). The molecular masses of the new variants correspond with those derived from the open reading frame analysis of the sequences. Interestingly, in the case of variants D and E, we detected minor additional bands approximately 4 kDa higher than the expected band. As glycosylation is the most common post-translational modification that can result in such an increase in molecular mass, we treated A549 cells over-expressing variants D and E either with the solvent or with the glycosylation inhibitor tunicamycin (2.5 μg/ml). Treatment of cells with glycosylation inhibitor resulted in disappearance of the additional band confirming glycosylation of variants D and E (Fig. 4B).

We also studied localization of HA-tagged Nox4 variant by immunostaining of the A549 cells over-expressing HA-tagged Nox4 variants using a HA antibody (Fig. 5). Staining of all variants was mainly detected in the cytoplasm and was enriched in the perinuclear area, whereas no staining was observed in the nucleus and the

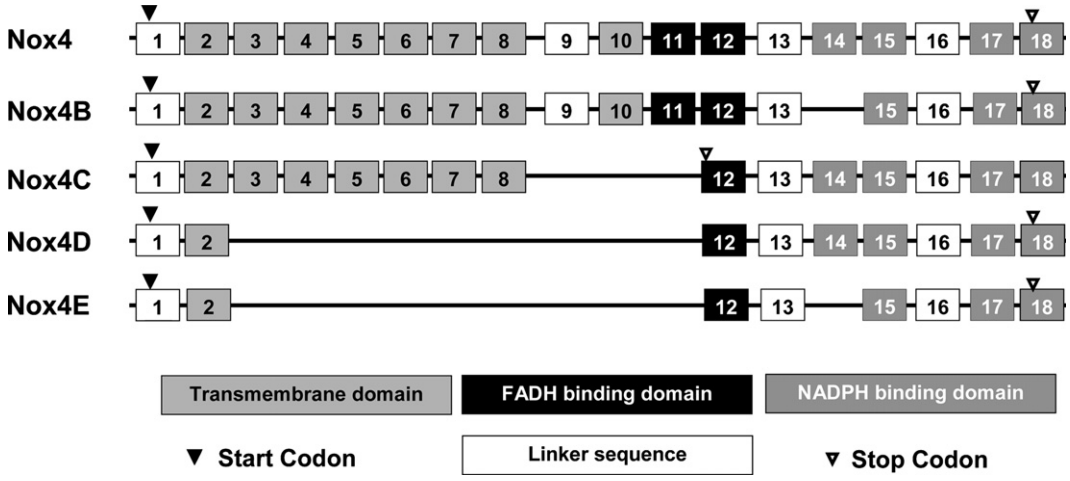

Fig. 2. Exon structure of newly identified Nox4 splice-variants compared to Nox4 prototype. The numbers in the boxes represent the exon number. The accession numbers of the sequences deposited in the EMBL database are as follows: variant B (AJ704726), variant C (AJ704727), variant D (AJ704728), and variant E (AJ704729).

plasma membrane. This differs from the bioinformatic analysis using PSORT II for prediction of sub-cellular localization (Table 1). For Nox4 prototype, variants B and C nearly 70% probability for association with endoplasmic reticulum was calculated. Since these variants also have the N-terminal hydrophobic domains, association with plasma membrane must also be considered. However, using PSORT II for Nox4 prototype only 11% probability for plasma membrane association was predicted, whereas no probability for plasma membrane association of variants B and C was predicted. For variants D and E, PSORT II predicted nearly 70% probability of being localized within the cytoplasm and not associated with membranes. In comparison, for Nox1 a much higher probability of 34% was predicted.

Generation of reactive oxygen species by Nox4 isoforms

Since NAD(P)H oxidases are ROS generating enzymes, it was of interest to investigate the effects of these variants on ROS generation. Thus, we performed ROS measurements in A549 cells over-expressing Nox4 variants. Since C-terminal tagged NAD(P)H oxidases were shown to have diminished activity, we employed non-tagged expression vectors for functional assays. In these experiments, Nox1 [10] was included as a control (Fig. 6A). As expected, the Nox1 and Nox4 prototype showed elevated ROS generation when compared with control vector. Variants B and C, which lack one or all NAD(P)H/FADH binding domains, exhibited reduced ROS concentration. The variant D that lacks transmembrane domains exhibited elevated ROS generation comparable with that observed for the Nox4 prototype. Variant E, which additionally lacks one NAD(P)H binding site, exhibited no change in ROS concentration.

Effect of glycosylation on Nox4D and Nox4E activity

As Nox4D and Nox4E were observed to be glycosylated, it was of interest to investigate the effect of glycosylation on the activity of these proteins. Inhibition of glycosylation by tunicamycin abrogated the increase in ROS due to Nox4D overexpression, while it had no effect in control cells as well as cells overexpressing Nox4E (Fig. 6B).

Discussion

In this study, we have analyzed the expression of Nox4 in human A549 cells. Western-blot analysis of A549 cells indicated several Nox4 immuno-reactive bands in addition to Nox4 prototype. Analysis of A549 mRNA by RT-PCR also indicated the presence of many smaller bands together with full length Nox4 described in the literature. Using shotgun-cloning and sequencing approach we identified three new Nox4 splice-variants and one variant similar to a previously documented NCBI database entry (AY288918) together with the full length Nox4. The presence of two independent database entries for Nox4 variants also gives a hint for the existence of differential splicing of Nox4 gene. Analysis of mRNA derived from lung homogenates, lung vessel preparations, primary cultured lung adventitial fibroblasts, and kidney HEK 293 cells by RT-PCR also revealed the presence of some of these variants.

Recently, a splice variant of Nox1 was described [22], which was later proved to be an artifact [23] due to template switching during cDNA synthesis. This Nox1 variant was not in agreement with the GT-AG splice rule and analysis of the sequence in the region of splicing

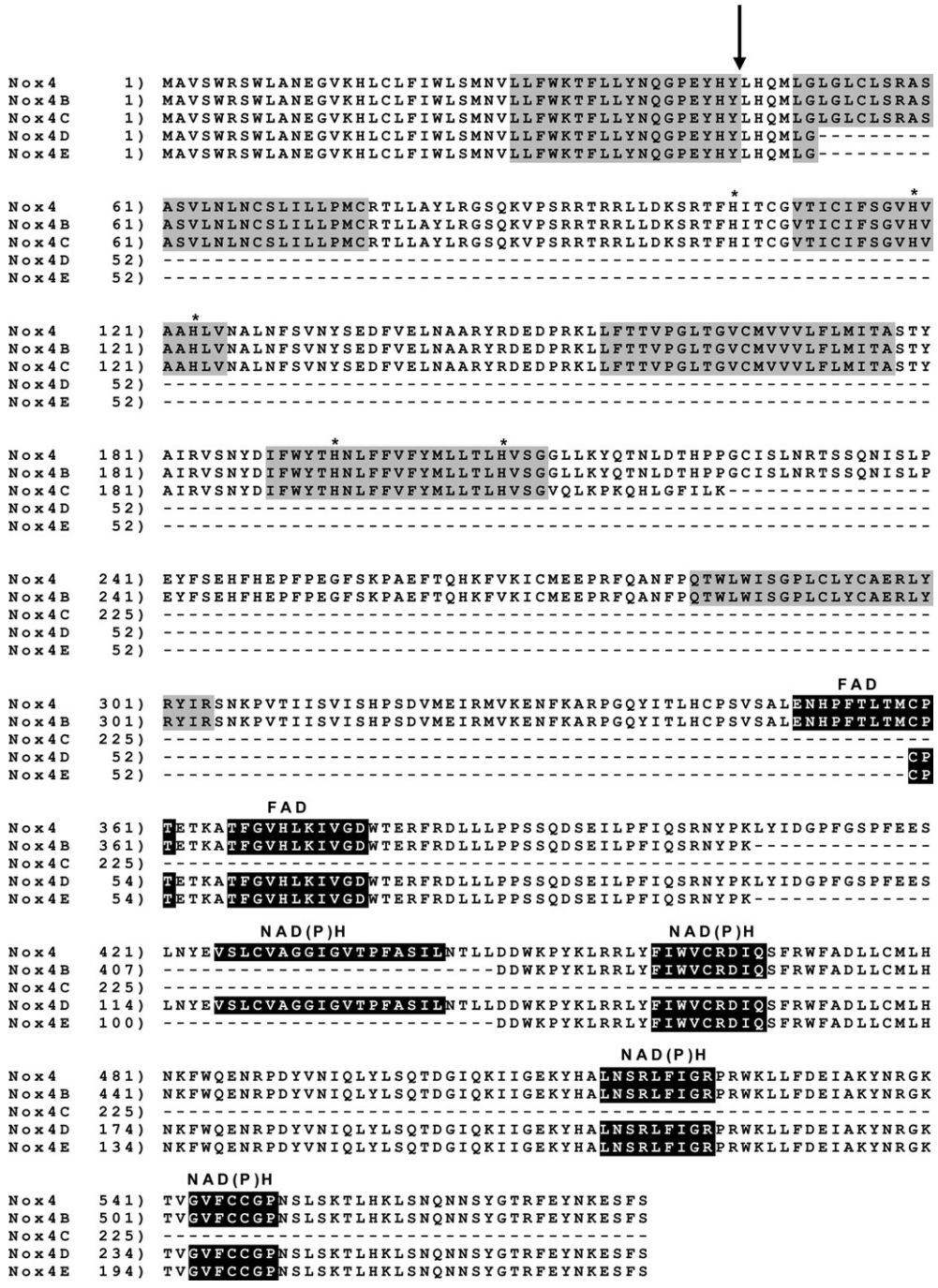

Fig. 3. The alignment of translated peptide sequences of the Nox4 prototype (Nox4) with identified Nox4 variants (Nox4B, Nox4C, Nox4D, and Nox4E). The arrow shows putative signal peptide cleavage site. Hydrophobic transmembrane domains are shown in gray. An asterisk shows conserved histidines representing putative iron/heme binding sites. FADH and NAD(P)H labeled black boxes represent FADH and NAD(P)H binding sites.

revealed the presence of repetitive sequence that resulted in template switching during cDNA synthesis. However, the splice variants of Nox4 as described in our study are in accordance with the GT-AG splice rule. Also, in these regions we could not detect any repetitive sequences that may result in template switching.

These Nox4 variants carry deletions in critical structural and functional domains. The Nox4 variants B and C lack the first NAD(P)H or all of the NAD(P)H and FAD binding sites. Both variants acted as dominant-negative molecules, since A549 cells transfected with these variants had lower ROS concentrations as compared to control plasmid transfected cells. Interestingly, this inhibitory effect on ROS generation was similar between variant B and C, thus indicating that the first NAD(P)H binding site has a strong impact on NAD(P)H

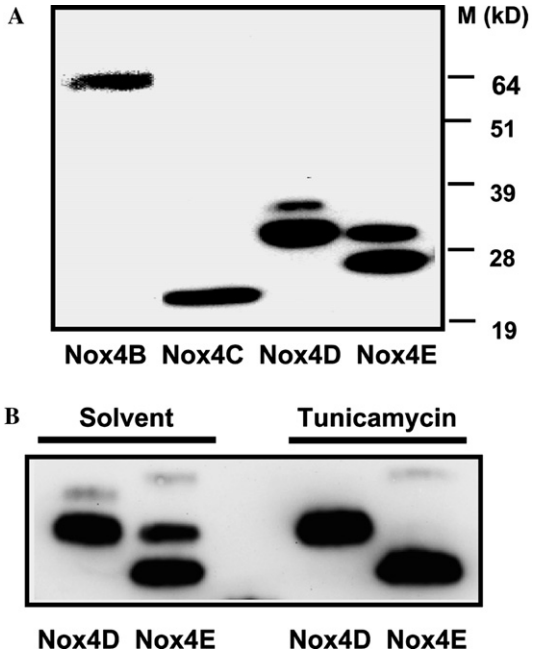

Fig. 4. (A) The HA-Western-blot analysis of A549 cells transfected with HA-tagged expression constructs fused to a cDNA encoding Nox4 splicing variants (Nox4B, Nox4C, Nox4D, and Nox4E). The molecular masses correspond to the predicted molecular masses from open reading frame analysis (Nox4B: 62.7 kDa, Nox4C: 25.7 kDa, Nox4D: 31.8 kDa, and Nox4E: 27.6 kDa, not including the additional 1.7 kDa molecular mass of HA-tag). (B) HA-Western blot analysis of A549 cells transfected with Nox4D or Nox4E, treated with either the solvent or the glycosylation inhibitor tunicamycin (2.5 μg/ml).

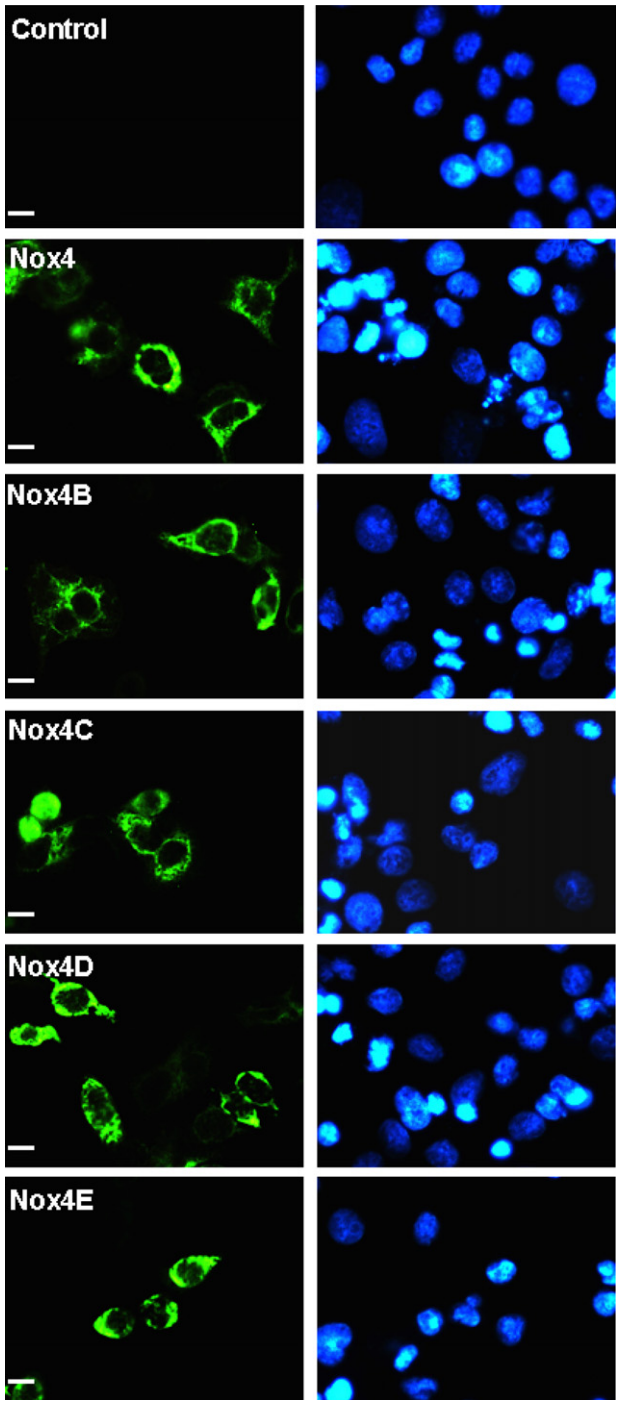

Fig. 5. HA immunocytochemical analysis of A549 cells transfected with HA-tagged expression constructs fused to a cDNA encoding Nox4 prototype (Nox4), Nox4 splicing variants (Nox4B, Nox4C, Nox4D, and Nox4E) or control (control vector). The left column represents HA staining (green). The right column represents corresponding nuclear DAPI staining (blue) = 20 μm. (For interpretation of the references to colour in this figure legend, the reader is referred to the web version of this paper.)

oxidase activity and cannot be fully compensated by the other NAD(P)H and FADH binding sites. The dominant-negative mechanism may be explained by the complexing of Nox4 with other subunits. The most likely candidate is $p22^{phox}$, which is co-localized with Nox4 [21], however other non-identified factors also have to be considered. A dominant-negative Nox4 isoform may competitively bind these factors rendering Nox4 inactive.

This observation is in line with a recent study, where a recombinant Nox4-encoding construct lacking the FADH/NAD(P)H oxidase-binding domains was demonstrated to be dominant- negative [24]. This dominant-negative form inhibited insulin stimulated H_2O_2 generation, demonstrating the role of Nox4 in this signaling process. In our study, we show that dominant-negative NAD(P)H oxidases are expressed endogenously. The function of endogenously expressed dominant-negative Nox4 variants is speculative. It may counterbalance specific intracellular signaling pathways. It may also have a protective function against ROS overloading of the cell or may contribute to the fine-tuning of ROS concentrations in specific sub-cellular compartments [21].

Two further variants, variants D and E, are described in this study that lack the hydrophobic putative transmembrane domains. Variants D and E are hence considered as soluble variants. When compared to variant D, variant E also lacks the first NAD(P)H oxidase-binding site, similar to variant B. Both of these variants were ob-

Table 1
Probability for sub-cellular localization of Nox4 prototype and Nox4 variants in comparison to Nox1 as analyzed by PSORT II software

	Endoplasmic reticulum (%)	Plasma membrane (%)	Nuclei (%)	Cytoplasm (%)
Nox4	67	11	—	—
Nox4B	78	—	—	—
Nox4C	67	—	—	—
Nox4D	—	—	17	70
Nox4E	—	—	17	70
Nox1	44	34	—	—

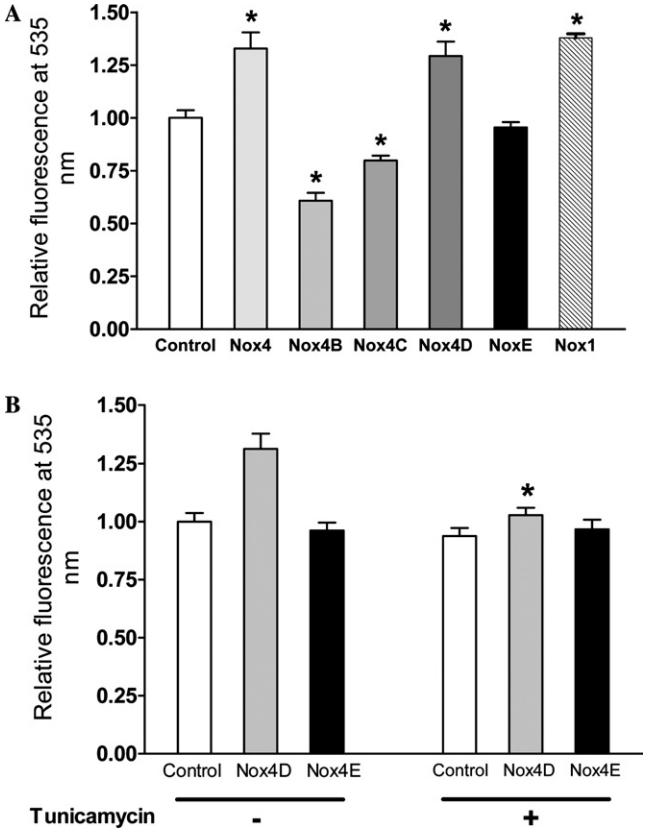

Fig. 6. (A) Measurement of ROS in A549 cells with the dichlorofluorescein technique. The A549 cells were transfected with control vector (control), or expression constructs for Nox4 prototype (Nox4), or Nox4 splice-variants (Nox4B, Nox4C, Nox4D, and Nox4E) or Nox1. ROS was measured 24 h after transfection. *Significant difference compared with control ($n = 6$, SEM, $p < 0.05$, Wilcoxon signed rank test). (B) The A549 cells were transfected with control vector (control), or expression constructs for Nox4 splice-variants Nox4D, or Nox4E and cultured in the presence or absence of tunicamycin (2.5 μg/ml). ROS was measured 24 h after transfection. *Significant difference compared with Nox4D cultured in absence of tunicamycin ($n = 6$, SEM, $p < 0.05$, Wilcoxon signed rank test).

served to be glycosylated. While variant D had an activity comparable to that of full length Nox4 prototype, variant E had no impact on cellular ROS concentration. Glycosylation of Nox4D was crucial for its activity as inhibition of glycosylation abrogated the inducing effects of Nox4D on ROS concentrations.

Of particular interest is variant D which lacks the transmembrane domains, apart from the first one however contains all NAD(P)H and FADH binding sites. This variant was shown to have NAD(P)H oxidase activity comparable to that of Nox4 prototype and is most likely a soluble NAD(P)H oxidase. Interestingly, this brings into question the necessity of conserved histidines distributed within the transmembrane containing N-terminus for enzymatic activity. These histidines are postulated to bind iron in complex with the heme group that is required for electron transfer to oxygen [25].

At present, it is not clear which additional subunits are indispensable in the soluble active Nox4 complex and if these subunits differ from those required for activity of the membrane bound Nox4 forms. A search for additional Nox4 binding partners is currently underway.

Sub-cellular localization of the presented Nox4 variants was studied using HA-tagged Nox4 variants. Tagging the protein allowed us to study the localization of Nox4 variants, which was not possible using our Nox4 antibody, since it could not detect variant C and could not distinguish between the Nox4 prototype, and variants B, D, and E. Immuno-staining of Nox4 variants using HA antibody indicated cytoplasmic and perinuclear expression, excluding the nuclei and the plasma membrane. No major differences were observed between soluble and membrane bound forms. One potential concern is that the over-expression of Nox4 variants will lead to overloading of the cell, making it difficult to localize the protein precisely at its final target. When performing bioinformatics analysis (PSORT II), we found high probabilities of Nox4 prototype, variants B and C to be associated with endoplasmic reticulum (ER), due to the presence of the ER retention signal represented by amino acids KESF. When performing this analysis on Nox4 variants D and E, which lack transmembrane domains, a high probability for cytoplasmic localization was calculated, supporting their soluble characteristics. These findings contrast with a study, which has shown prominent Nox4 expression within the nucleus of vascular smooth muscle cells [21].

The existence of different Nox4 isoforms and Nox1 within the same cell as found for A549 cells [10] questions their function. One possible reason could be that the subcellular targeting of Nox isoforms may represent different site-specific requirements of ROS. Compartmentalized generation of ROS, which have a rather short half-life, may be of importance for their role in cellular signaling.

The occurrence of the newly discovered Nox4 variants is of interest for the mechanism of NAD(P)H oxidase regulation. Regulation of NAD(P)H oxidases by phosphorylation is well documented. The cytosolic proteins $p47^{phox}$, $p67^{phox}$, $p40^{phox}$, and the small G-protein rac translocate to the cell membrane and interact with

flavocytochrome b558 upon cell activation. Cell activation can occur by protein kinase C-dependent phosphorylation of $p47^{phox}$. In addition, relevant protein kinase A, PI3 kinase, and MAP-kinase phosphorylation sites may also play a role [21]. In the context of the findings reported in this study, a regulatory role for the newly discovered Nox4 isoforms on overall Nox activity can be considered. Differential splicing may contribute to the control of compartmentalized ROS generation and related signaling.

Taken together, we describe the isolation and characterization of four new Nox4 isoforms that lack different structural domains, which alter their intracellular trafficking and regulate ROS generation.

Acknowledgments

Parag Goyal is supported by a predoctoral fellowship from ALTANA Pharma. The authors thank Dr. Rory Morty for critical reading of the manuscript. This work was supported by the Deutsche Forschungsgemeinschaft SFB 547, Project B7 and B9.

References

[1] B.M. Babior, Oxygen-dependent microbial killing by phagocytes, Engl. J. Med. 298 (1978) 659–668.
[2] T.G. Gabig, R.S. Kipnes, B.M. Babior, Solubilization of the O_2 (−)-forming activity responsible for the respiratory burst in human neutrophils, J. Biol. Chem. 253 (1978) 6663–6665.
[3] T.L. Dawson, G.J. Gores, A.L. Nieminen, B. Herman, J.J. Lemasters, Mitochondria as a source of reactive oxygen species during reductive stress in rat hepatocytes, Am. J. Physiol. 264 (1993) C961–C967.
[4] S.A. Sanders, V. Massey, The thermodynamics of xanthine oxidoreductase catalysis, Antioxid. Redox Signal. 1 (1999) 371–379.
[5] W. Wang, S. Wang, L. Yan, P. Madara, P.C.A. Del, R.A. Wesley, R.L. Danner, Superoxide production and reactive oxygen species signaling by endothelial nitric-oxide synthase, J. Biol. Chem. 275 (2000) 16899–16903.
[6] V.J. Thannickal, B.L. Fanburg, Reactive oxygen species in cell signaling, Am. J. Physiol. Lung Cell. Mol. Physiol. 279 (2000) L1005–L1028.
[7] T. Porwol, W. Ehleben, V. Brand, H. Acker, Tissue oxygen sensor function of NAD(P)H oxidase isoforms, an unusual cytochrome aa3 and reactive oxygen species, Respir. Physiol. 128 (2001) 331–348.
[8] M.S. Wolin, T.M. Burke-Wolin, H.K.M. Mohazzab, Roles for NAD(P)H oxidases and reactive oxygen species in vascular oxygen sensing mechanisms, Respir. Physiol. 115 (1999) 229–238.
[9] Y.M. Go, J.J. Gipp, R.T. Mulcahy, D.P. Jones, H_2O_2-dependent activation of GCLC-ARE4 reporter occurs by mitogen-activated protein kinase pathways without oxidation of cellular glutathione or thioredoxin-1, J. Biol. Chem. 279 (2004) 5837–5845.
[10] P. Goyal, N. Weissmann, F. Grimminger, C. Hegel, L. Bader, F. Rose, L. Fink, H.A. Ghofrani, R.T. Schermuly, H.H. Schmidt, W. Seeger, J. Hänze, Upregulation of NAD(P)H oxidase 1 in hypoxia activates hypoxia-inducible factor 1 via increase in reactive oxygen species, Free Radic. Biol. Med. 36 (2004) 1279–1288.
[11] N.S. Chandel, D.S. McClintock, C.E. Feliciano, T.M. Wood, J.A. Melendez, A.M. Rodriguez, P.T. Schumacker, Reactive oxygen species generated at mitochondrial complex III stabilize hypoxia-inducible factor-1alpha during hypoxia: A mechanism of O_2 sensing, J. Biol. Chem. 275 (2000) 25130–25138.
[12] Y. Ohara, T.E. Peterson, D.G. Harrison, Hypercholesterolemia increases endothelial superoxide anion production, J. Clin. Invest. 91 (1993) 2546–2551.
[13] B. Tesfamariam, R.A. Cohen, Free radicals mediate endothelial cell dysfunction caused by elevated glucose, Am. J. Physiol. 263 (1992) H321–H326.
[14] J.B. Laursen, S. Rajagopalan, Z. Galis, M. Tarpey, B.A. Freeman, D.G. Harrison, Role of superoxide in angiotensin II-induced but not catecholamine-induced hypertension, Circulation 95 (1997) 588–593.
[15] Y.A. Suh, R.S. Arnold, B. Lassegue, J. Shi, X. Xu, D. Sorescu, A.B. Chung, K.K. Griendling, J.D. Lambeth, Cell transformation by the superoxide-generating oxidase Mox1, Nature 401 (1999) 79–82.
[16] G. Cheng, Z. Cao, X. Xu, E.G. van Meir, J.D. Lambeth, Homologs of gp91phox: cloning and tissue expression of Nox3, Nox4, and Nox5, Gene 269 (2001) 131–140.
[17] D. Rotrosen, C.L. Yeung, J.P. Katkin, Production of recombinant cytochrome b558 allows reconstitution of the phagocyte NAD(P)H oxidase solely from recombinant proteins, J. Biol. Chem. 268 (1993) 14256–14260.
[18] B.M. Babior, The respiratory burst oxidase, Curr. Opin. Hematol. 2 (1995) 55–60.
[19] A. Shiose, J. Kuroda, K. Tsuruya, M. Hirai, H. Hirakata, S. Naito, M. Hattori, Y. Sakaki, H. Sumimoto, A novel superoxide-producing NAD(P)H oxidase in kidney, J. Biol. Chem. 276 (2001) 1417–1423.
[20] B. Banfi, R.A. Clark, K. Steger, K.H. Krause, Two novel proteins activate superoxide generation by the NAD(P)H oxidase NOX1, J. Biol. Chem. 278 (2003) 3510–3513.
[21] L.L. Hilenski, R.E. Clempus, M.T. Quinn, J.D. Lambeth, K.K. Griendling, Distinct subcellular localizations of Nox1 and Nox4 in vascular smooth muscle cells, Arterioscler. Thromb. Vasc. Biol. 24 (2004) 677–683.
[22] B. Banfi, A. Maturana, S. Jaconi, S. Arnaudeau, T. Laforge, B. Sinha, E. Ligeti, N. Demaurex, K.H. Krause, A mammalian H^+ channel generated through alternative splicing of the NADPH oxidase homolog NOH-1, Science 287 (2000) 138–142.
[23] M. Geiszt, K. Lekstrom, T.L. Leto, Analysis of mRNA transcripts from the NAD(P)H oxidase 1 (Nox1) gene: Evidence against production of the NADPH oxidase homolog-1 short (NOH-1S) transcript variant, J. Biol. Chem. 279 (2004) 51661–51668.
[24] K. Mahadev, H. Motoshima, X. Wu, J.M. Ruddy, R.S. Arnold, G. Cheng, J.D. Lambeth, B.J. Goldstein, The NAD(P)H oxidase homolog Nox4 modulates insulin-stimulated generation of H_2O_2 and plays an integral role in insulin signal transduction, Mol. Cell. Biol. 24 (2004) 1844–1854.
[25] J.D. Lambeth, Regulation of the phagocyte respiratory burst oxidase by protein interactions, J. Biochem. Mol. Biol. 33 (2000) 427–439.